Probing the Influence of Polymer Architecture on Liquid−Liquid Phase Transitions of Aqueous Poly(*N,N*-dimethylacrylamide) Copolymer Solutions

Xiangchun Yin and Harald D. H. Stöver*

Department of Chemistry, McMaster University, Hamilton, Ontario, Canada L8S 4M1

Received June 10, 2004; Revised Manuscript Received January 10, 2005

ABSTRACT: Thermosensitive poly(*N,N*-dimethylacrylamide-*co*-*N*-phenylacrylamide) (DMA-*co*-PhAm) copolymers were prepared by atom transfer radical polymerization (ATRP) in methanol/water mixtures at room temperature with methyl 2-chloropropionate as the initiator and CuCl/Me_6TREN as the catalyst. The resultant DMA-*co*-PhAm copolymers had tailored compositions and controlled molecular weights, and their aqueous solutions underwent liquid−liquid phase separation upon heating. These phase transition temperatures, measured by the cloud point method, were dependent on polymer concentrations, compositions, and molecular weights. The efficiency of the thermally induced liquid−liquid phase transition, i.e., the yield of phase-separated polymer, increased with increasing solution temperature, suggesting this thermally induced liquid−liquid phase transition to be a continuous equilibrium process. The efficiency of phase separation could be enhanced by adding NaCl to the solution.

Introduction

The liquid−liquid phase transitions of aqueous polymer solutions have been widely used in biochemistry and biotechnology for purifications of amino acids, proteins, nucleic acids, and cells.[1−3] Because of the fairly high water content even in the polymer-rich phase, such liquid−liquid phase transitions permit the separation of biomaterials without denaturation. Classical examples include the dextran/poly(ethylene glycol) and poly(ethylene glycol)/salts systems.[4−6] Recently, the thermally induced liquid−liquid phase transition of aqueous polymer solutions has gained increasing attention for similar reasons.[7,8] These aqueous polymer solutions are characterized by a lower critical solution temperature (LCST), above which the polymer becomes insoluble.

Thermally induced liquid−liquid phase transitions are commonly seen in biomacromolecules such as elastin-like polypeptides and have been used to purify recombinant proteins from the cell lysate.[9−11] The most studied thermoresponsive polymer is poly(*N*-isopropylacrylamide) (pNIPAM), which undergoes a liquid−solid phase transition near its LCST of around 32 °C.[12] In contrast, aqueous solutions of the more polar poly(*N,N*-dimethylacrylamide) (pDMA) do not show LCST behavior. However, aqueous solutions of DMA copolymers containing hydrophobic comonomers that enhance polymer−polymer interactions are again thermally responsive. Unlike pNIPAM, however, these DMA copolymers tend to undergo liquid−liquid phase transitions, with the phase transition temperature depending on the amount of hydrophobic comonomer.[13−15]

We have studied the thermally induced liquid−liquid phase transitions of aqueous solutions of pDMA copolymers and used their liquid−liquid phase transition to prepare cross-linked hydrogel microspheres.[16,17] We found that the yield of phase-separated polymers was typically less than 10% at the onset of phase separation and increased with increasing temperatures. Despite extensive studies on thermally responsive polymers, there appears to be little information available on the efficiency of such liquid−liquid phase separations. This efficiency should depend on the average composition and the compositional distribution as well as on the molecular weight and the molecular weight distribution of the copolymers. Most thermally responsive polymers studied to date were prepared by conventional radical polymerization, with correspondingly little control over molecular weight and molecular weight distribution.

Controlled/living radical polymerization, in particular atom transfer radical polymerization (ATRP), has been extensively used to prepare well-defined polymers with comb, star, and dendritic morphologies as well as random, gradient, and blocky comonomer sequences.[18] In the present work, we report the synthesis of well-defined random copolymers of *N,N*-dimethylacrylamide (DMA) with *N*-phenylacrylamide (PhAm) and their aqueous solution properties. The PhAm is added to increase the hydrophobicity of the copolymer and permit thermally induced phase separations. The primary objective of this research is to probe the mechanism of the thermally induced liquid−liquid phase transition using copolymers with well-defined structures.

Experimental Section

Materials. *N,N*-Dimethylacrylamide (DMA, 99%), aniline (99%), acryloyl chloride (96%), triethylamine (99%), tris(2-aminoethyl)amine (96%), methyl 2-chloropropionate (MCP) (97%), copper(I) chloride (>99%), and silica gel (100−200 mesh, column chromatography grade) were purchased from Aldrich. Methanol (HPLC grade), distilled water (HPLC grade), tetrahydrofuran (THF), dimethylformamide (DMF), methylene chloride, and anhydrous diethyl ether were obtained from Caledon Laboratories. DMA was purified by vacuum distillation, while other materials were used as received. Tris(2-(dimethylamino)ethyl)amine (Me_6TREN) was synthesized according to a literature procedure.[19]

Synthesis of *N*-Phenylacrylamide (PhAm). Aniline (36.9 mL, 0.4 mol) and triethylamine (84.5 mL, 0.6 mol) were dissolved in 200 mL of methylene chloride. Acryloyl chloride (25.4 mL, 0.3 mol) dissolved in 15 mL of methylene chloride was added dropwise to this well-stirred solution at 0 °C. The

* Corresponding author. E-mail stoverh@mcmaster.ca.

10.1021/ma048853p CCC: $30.25
Published on Web 02/19/2005

mixture was then warmed to room temperature and stirred for another 4 h. The reaction solution was filtered, washed three times with water, and dried over anhydrous magnesium sulfate. The solvent was removed on a rotary evaporator to yield a deep yellow solid that was recrystallized from acetone and dried under vacuum to afford 22.0 g of PhAm (yield, 50%). ^{1}H NMR (methylene chloride-d_2) at 300 MHz: 7.0−7.7 ppm (m, 5H, arom), 6.3−6.4 ppm (m, 2H, CH_2 vinyl), 5.7−5.8 ppm (dd, 1H, CH vinyl).

ATRP of DMA and PhAm. DMA, methanol, and water were purged with nitrogen for 30 min before use. In a typical procedure, a 50 mL flask was first flushed with nitrogen for about 1 h. A solution comprised of DMA (7.83 g, 0.079 mol), PhAm (3.38 g, 0.023 mol), methanol (8.97 g), water (2.24 g), and copper(I) chloride (25.3 mg, 2.55×10^{-4} mol) was transferred to the flask under nitrogen. Me_6TREN (68 μL, 2.55×10^{-4} mol) was added with a syringe, and the flask was placed into a water bath. After stirring the mixture for 10 min, MCP (30.7 μL, 2.55×10^{-4} mol) was added. The polymerization was carried out at room temperature. During the polymerization, 1.0 mL aliquots were withdrawn at different times with a degassed syringe for molecular weight and conversion measurements. The molecular weight of the polymers was measured after diluting 0.2 mL of the sample with THF and passing this mixture through a short silica column to remove the catalyst. Conversion was determined gravimetrically by precipitating 0.8 mL of the aliquot into 20 mL of diethyl ether. The polymer was isolated by centrifugation and dried under vacuum at 65 °C. Only residual monomer was left after the precipitation as confirmed by ^{1}H NMR. Precipitation was quantitative as verified by repeat precipitations. Samples for the phase transition study similarly diluted with THF and passed through a silica column to remove the catalyst. The polymer was precipitated into diethyl ether, redissolved in acetone, reprecipitated into diethyl ether, and then dried under vacuum at 65 °C.

Characterization of Copolymers. Molecular weights of copolymers were determined using a gel permeation chromatograph consisting of a Waters 515 HPLC pump, three UltraStyragel columns (500−20K, 500−30K, 5K−600K Da), and a Waters 2414 refractive index detector, using THF as solvent at a flow rate of 1 mL min^{-1}, and narrow-disperse polystyrene as calibration standards. ^{1}H NMR spectra of the copolymers were recorded on Bruker AC 200 and Bruker AC 300 NMR spectrometers, using methylene-d_2 chloride as the solvent.

Measurement of Phase Transition Temperatures. Phase transition temperatures of aqueous solutions of DMA-*co*-PhAm copolymers were measured using the cloud point method. A Cary 100 Bio UV−vis spectrophotometer, coupled with a temperature controller, was used to trace the phase transition by monitoring the transmittance at 500 nm. The phase transition temperature was defined as the inflection point of the transmittance vs temperature curve, as determined by the maximum in the first derivative. The polymer concentration and the heating rate were 1 wt % and 1.0 °C min^{-1}, respectively.

Liquid−liquid Phase Transition of DMA-*co*-PhAm Copolymer Solutions. Optical images of polymer solutions at temperatures above or below the phase transition temperature were recorded using an Olympus BH-2 microscope equipped with a Kodak DC 120 Zoom digital camera.

To measure the efficiency of the phase separation, 20 g of a 2.0 wt % aqueous solution of DMA-*co*-PhAm22, containing 22 mol % PhAm, was prepared in a 24 mL glass vial. The solution was incubated in a temperature-controlled water bath at 25 °C for 30 min. The resulting two-phase mixture was then separated by centrifugation at 3500 rpm for 1 min into a viscous coacervate bottom phase and a transparent supernatant, which were then isolated by decanting the supernatant into a pan. Both phases were dried to constant weight at 65 °C.

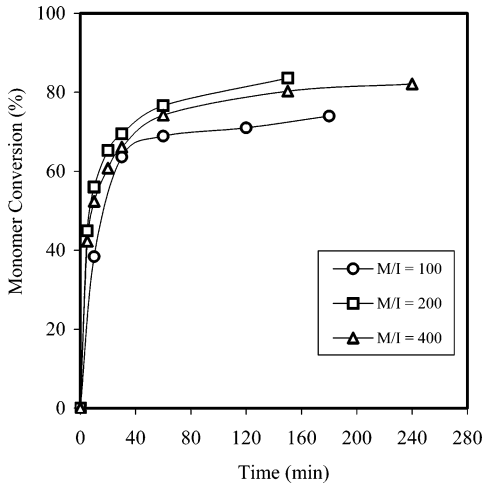

Figure 1. Conversion vs time for the ATRP of *N,N*-dimethylacrylamide in methanol at room temperature under three different monomer/initiator (M/I) ratios. Monomer/solvent = 1/2 (w/w), [CuCl]/[Me_6TREN]/[2-chloropropionate] = 1/1/1. The solid lines connecting the data points are only to guide the eye.

Results and Discussion

ATRP of DMA in Methanol Solution. The controlled polymerization of DMA by ATRP is difficult, plausibly due to three reasons: (1) the deactivation of the ATRP catalyst by binding to monomeric or polymeric amide groups, (2) the substitution of halide from the propagating chain ends by amide, and (3) the low values of the ATRP equilibrium constant.[20,21] Such challenges in the ATRP of DMA were addressed by using stronger ATRP coordinating ligands and more stable alkyl chlorides as initiators.[22,23] The best system reported to date uses the powerful ATRP catalyst CuCl/Me_6TREN and methyl 2-chloropropionate (MCP) as initiator; however, high monomer conversions (up to 70%) were only obtained with high catalyst-to-initiator ratios (2/1 or 3/1).[23]

Our initial studies concentrated on further improving the ATRP of DMA by exploring the effects of solvents on the polymerization. With CuCl/Me_6TREN as the catalyst and MCP as the initiator in a 1:1:1 ratio, the polymerization proceeded initially very rapidly in ethyl acetate, THF, and DMF but stopped within 5−10 min at room temperature at less than 20% monomer conversions. The polymerization proceeded more slowly in toluene to reach about 40% monomer conversion after 20 h. In ethyl acetate, THF, and toluene, blue precipitates were formed during the polymerization. In all cases, the molecular weight distributions were below 1.1, indicating the polymerizations were well controlled. In addition, the polymerizations continued upon adding fresh catalyst. It hence appears that catalyst deactivation is still a major problem in ATRP of DMA, even with CuCl/Me_6TREN as the catalyst. Assuming that the amide groups of DMA or pDMA displace chloride from the catalyst, and then using a hydrogen-bonding solvent such as an alcohol to bind to the amide groups, might prevent this deactivation. Similar approaches have been used in the ATRP of the strongly coordinating monomer, vinylpyridine.[24]

Figures 1 and 2 depict typical curves for monomer conversion vs time and molecular weight vs conversion, for the ATRP of DMA in methanol in a water bath at room temperature, with CuCl/Me_6TREN as the catalyst

Table 1. Synthesis of Poly(DMA-*co*-PhAm) by ATRP at Room Temperature in Different Solvents[a]

			mol % PhAm					
entry	solvent	monomer/solvent[b]	in feed	in polymer[c]	conv (%)	M_n^{theo}	M_n[d]	M_w/M_n[d]
I	MeOH	2/1	9.8	9.9	57	23600	6800	1.07
II	MeOH/H_2O (9/1)[b]	2/1	9.8	9.8	69	28600	8200	1.07
III	MeOH/H_2O (9/1)	1/1	9.8	9.6	82	34000	9700	1.07
IV	MeOH/H_2O (9/1)	1/1	12.7	12.2	60	25200	7900	1.07
V	MeOH/H_2O (4/1)	1/1	12.7	12.0	80	33600	10100	1.09
VI	MeOH/H_2O (4/1)	1/1	16.7	15.9	76	32500	10200	1.07
VII	MeOH/H_2O (4/1)	1/1	22.5	21.7	70	30700	8600	1.07

[a] [Monomer]/[2-chloropropionate]/[CuCl]/[Me_6TREN] = 400/1/1/1; reaction time, 4 h. [b] The ratios are by weight. [c] Measured by ^{1}H NMR. [d] Measured by GPC.

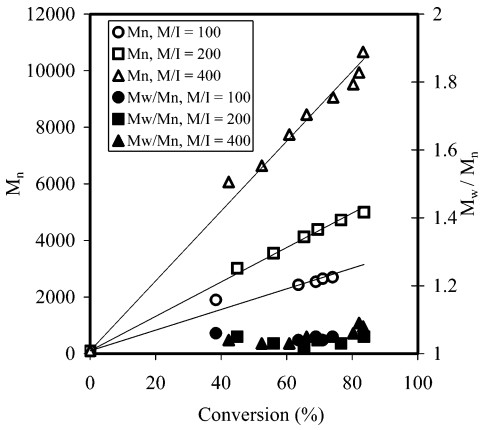

Figure 2. Plots of molecular weight, M_n (GPC), and molecular weight distribution, M_w/M_n, vs monomer conversion for the polymerization of *N*,*N*-dimethylacrylamide in methanol at room temperature under three different monomer/initiator (M/I) ratios. Monomer/solvent = 1/2 (w/w), [CuCl]/[Me_6TREN]/[2-chloropropionate] = 1/1/1. The solid lines are first-order trendlines.

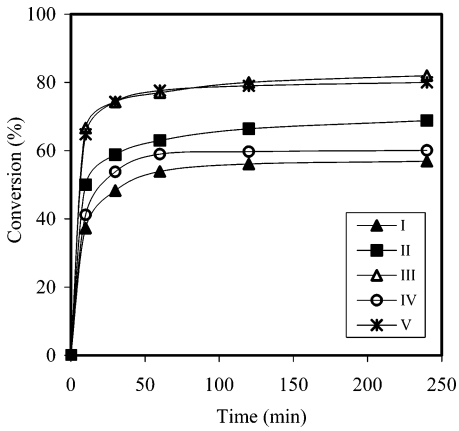

Figure 3. Conversion vs time curves for the ATRP of *N*,*N*-dimethylacrylamide and phenylacrylamide in methanol/water mixture at room temperature. Reaction conditions are those in Table 1. The solid lines connecting the data points are only to guide the eye.

and MCP as the initiator (1:1:1). The polymerization is rapid at the beginning, leading to 50% monomer conversion within 30 min and 80% after 4 h, while maintaining good control over the molecular weight distributions (M_w/M_n < 1.1). In addition, no catalyst precipitates during the polymerization. These results support the hypothesis that H-bonding solvents are suitable reaction media for the controlled ATRP of DMA.

The molecular weights of polymers determined by GPC and shown in Figure 2 deviate from the theoretical molecular weights, presumably due to the calibration method involving narrow disperse polystyrene standards. The molecular weights of pDMA from GPC are hence underestimated, though the trends are considered reliable.

While this work was being carried out, Matyjaszewski's group disclosed results on the ATRP of DMA in methanol solution with the addition of Lewis acids to control the stereochemistry of the polymers.[25] Under their conditions, the monomer conversion was less than 50% in the presence of Lewis acid.

ATRP Copolymerization of DMA and PhAm in Methanol/Water Mixtures. We next turned to the copolymerization of DMA with PhAm in analogous methanol solutions. Addition of 9.8 mol % PhAm led to narrow-disperse copolymer, but in only 57% yield (Table 1, entry I, and Figure 3, curve I). It appears that the added PhAm lowers the catalyst activity or catalyst lifetime, by changing the solvency of the reaction medium and/or by coordinating to the catalyst. We hence added water as a very polar cosolvent in order to increase the catalyst activity, in accordance with previous reports.[26,27]

The polymer yield increases to 69% in 90/10 (w/w) methanol/water mixtures (Table 1-II and Figure 3-II) and further to 82% in by increasing the monomer/solvent ratio to 1:1 (w/w) (Table 1-III and Figure 3-III). Under the same conditions, the yield drops to 60% when increasing PhAm to 12.7 mol % (Table 1-IV and Figure 3-IV) but recovers back to 80% upon changing the polymerization medium to 80/20 (w/w) methanol/water (Table 1-V and Figure 3-V). Several other DMA-*co*-PhAm copolymers with different compositions and different molecular weights were prepared by ATRP in 80/20 (w/w) methanol/water mixtures (Tables 1 and 2). All polymers have narrow molecular weight distributions, indicating that water improves the activity of catalysts without noticeably influencing the control of polymerizations. It is currently not clear that such enhancement of catalyst activity is due to water changing the catalyst structure[26] or due to water preventing the binding of amide to the catalyst.

A typical ^{1}H NMR spectrum of DMA-*co*-PhAm copolymer is presented in Figure 4. The copolymer composition was determined by comparing the peak area of the phenyl protons (5 H) from PhAm, with the total peak area between 2.3 and 3.3 ppm, which includes seven protons (a, c) from DMA and one proton (e) from PhAm. The results are illustrated in Tables 1 and 2. On the basis of the free radical reactivity ratios of DMA and PhAm reported in the literature,[14] it is expected that the monomer units are randomly distributed in the polymer chains. As shown in Tables 1 and 2, the compositions of the copolymers are close to the monomer feed ratio at all monomer conversions.

Thermally Induced Liquid−liquid Phase Transitions of DMA-*co*-PhAm Copolymer Solutions. The

Table 2. Synthesis of Poly(DMA-*co*-PhAm) with Different Molecular Weights via ATRP in 80/20 (w/w) Methanol/Water Mixtures at Room Temperature[a]

	mol % PhAm						
[monomer]/[MCP]	in feed	in polymer[b]	conv (%)	M_n^{theo}	M_n[c]	M_w/M_n[c]	cloud point[d] (°C)
60/1	16.7	15.9	89	5700	2000	1.08	39.3
100/1	16.7	16.2	84	9000	3500	1.06	40.2
200/1	16.7	16.3	77	16500	4700	1.05	39.1
400/1	16.7	15.9	76	32500	10200	1.07	43.5
100/1	22.5	21.8	80	8800	3200	1.07	16.3
200/1	22.5	21.7	73	16000	4600	1.07	17.2
400/1	22.5	21.7	70	30700	8600	1.07	20.1
600/1	22.5	22.0	61	40200	10600	1.07	20.1

[a] [CuCl]/[Me_6TREN]/[2-chloropropionate] = 1/1/1; monomer/solvent = 1/1 (w/w); reaction time, 4 h. [b] Measured by ^{1}H NMR. [c] Measured by GPC. [d] 1.0 wt % polymer solution.

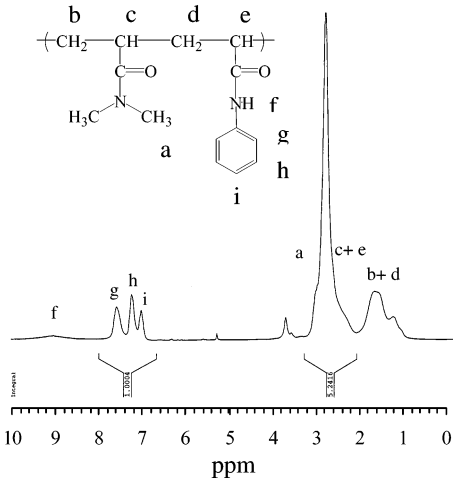

Figure 4. ^{1}H NMR spectrum of poly(DMA-*co*-PhAm22) in methylene-d_2 chloride.

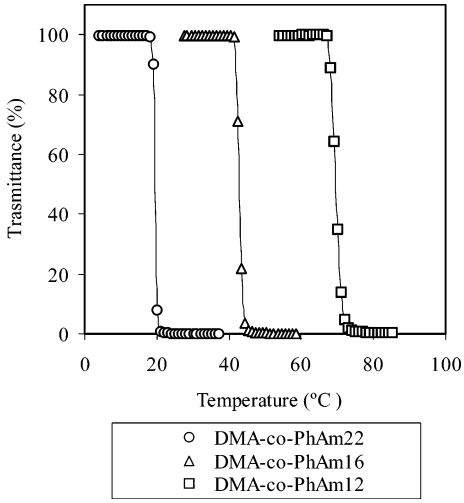

Figure 5. Cloud point curves for 1.0 wt % aqueous solutions of DMA-*co*-PhAm copolymers with different compositions.

temperature-dependent phase separation of aqueous solutions of DMA-*co*-PhAm copolymers was investigated by the cloud point method. Figure 5 shows the transmittance vs temperature curves for three DMA-*co*-PhAm copolymers with different compositions. The copolymer characteristics and their corresponding cloud point temperatures are given in Table 3.

The cloud point temperature of thermally responsive polymers is strongly influenced by changes in the hydrophilic/hydrophobic nature of the polymer. Aqueous solutions of DMA-*co*-PhAm copolymers with less than 10 mol % PhAm do not show a cloud point. With increasing PhAm content, the cloud point temperature

Table 3. Compositions and Phase Transition Temperatures of DMA-*co*-PhAm Copolymers

polymer	PhAm in polymer (mol %)[a]	M_n^{theo}	M_n[b]	M_w/M_n[b]	cloud point[c] (°C)
DMA-*co*-PhAm10	9.6	34000	9700	1.07	
DMA-*co*-PhAm12	12.0	33600	10100	1.09	70.1
DMA-*co*-PhAm16	15.9	32500	10200	1.07	43.5
DMA-*co*-PhAm22	21.7	30700	8600	1.07	20.1

[a] Estimated by NMR. [b] Measured by GPC. [c] Measured by the cloud point method with 1.0 wt % polymer solution.

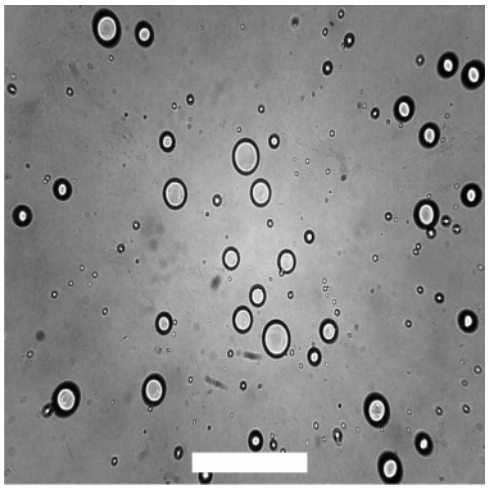

Figure 6. Optical microscope image of liquid droplets formed from the phase transition of 1 wt % DMA-*co*-PhAm22 solution at 25 °C. Scale bar is 250 μm.

decreases drastically (Table 3). It is thought that the phase separation of such polymers is caused by the presence of hydrophobic groups in the polymer chains.[28−30] At low temperature, strong hydration of the hydrophilic groups dissolves the polymer and hence forces entropically unfavorable structuring of water around the hydrophobic groups. Above the phase transition temperature, the now dominant entropy gain drives the dissociation of this water from the polymer and leads to a negative free energy of desolvation. An increase in hydrobicity of the polymer increases the entropic penalty from this structured water, lowers the enthalpy gained from solvating the hydrophilic units, and hence decreases the cloud point.

The thermally induced phase separation observed in aqueous DMA-*co*-PhAm copolymer solution is a liquid−liquid transition. Figure 6 presents an optical microscope image of the liquid coacervate droplets formed from a 1.0 wt % aqueous DMA-*co*-PhAm22 solution. In the absence of stirring, these droplets will coalesce into a bulk layer after several minutes.

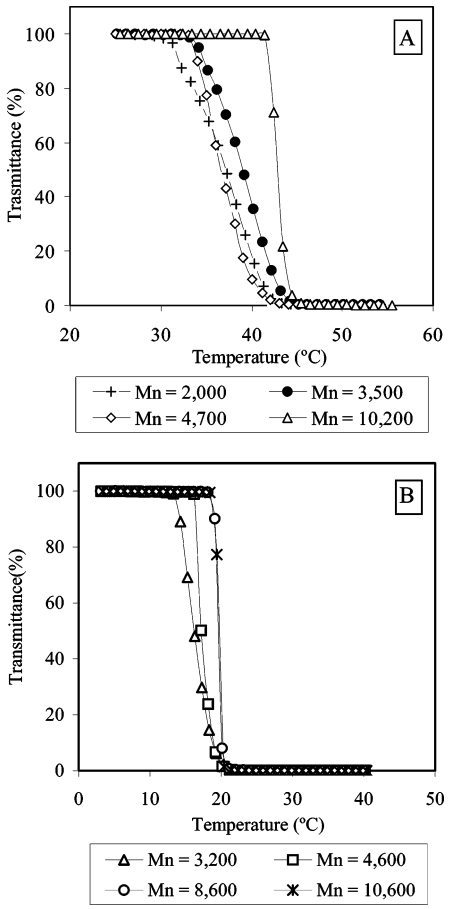

Figure 7. Effects of polymer molecular weights on the phase transition temperature of 1.0 wt % DMA-*co*-PhAm copolymer solutions. The PhAm content in the copolymer is about (A) 16 mol % and (B) 22 mol %. The molecular weights indicated are measured by GPC (see Table 2).

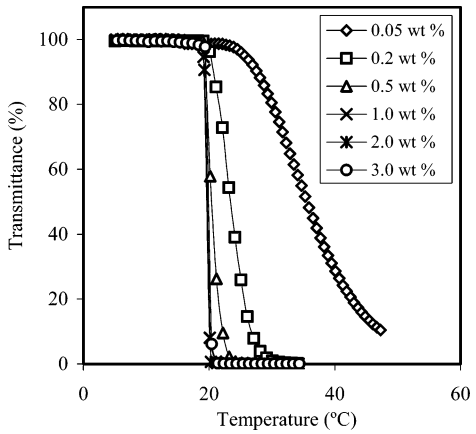

Figure 8. Cloud point curves for aqueous solutions of DMA-*co*-PhAm22 with different concentrations.

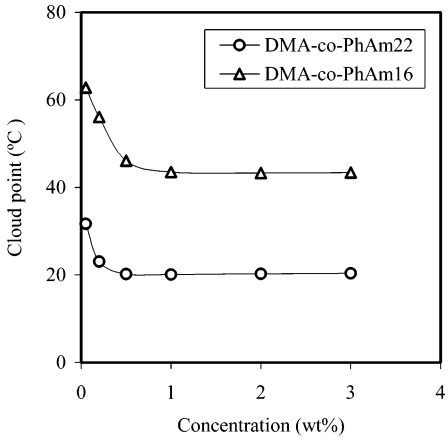

Figure 9. Effect of polymer concentration on the phase separation temperature of DMA-*co*-PhAm solutions as measured by the cloud point method.

Because of the difficulty in obtaining thermally responsive polymers with narrow molecular weight distributions, the dependence of LCST on the molecular weight of polymers has not been systematically studied. For example, Fujishige et al. reported the LCST of pNIPAM to be independent of chain length for molecular weights larger than 50 000,[31] while Schild and Tirrell indicated a small effect of molecular weight on the LCST of pNIPAM.[32] The pNIPAM used in both studies was prepared by conventional radical polymerization and had broad molecular weight distributions. Using fractionated pNIPAMs with narrow molecular weight distributions, Tong et al. reported that the LCST of pNIPAM increases with molecular weight.[33]

Figure 7 illustrates the effect of molecular weight on the cloud point of two series of DMA-*co*-PhAm copolymers, containing 16% and 22% PhAm. The phase transition temperatures first increase slightly with increasing molecular weight and then become constant (Figure 7B). The polymers with lower molecular weights show phase transitions over relatively broad temperature ranges. This may be due small compositional variations or due to the influence of the initiating methoxypropionate group. Both of these effects would be more pronounced at lower molecular weights.

Effects of Polymer Concentration and Added NaCl on the Phase Transition Temperatures. Figures 8 and 9 show the effects of polymer concentration on the cloud point curves for DMA-*co*-PhAm22 and on the cloud point temperatures for two copolymer compositions, respectively. The cloud point temperatures initially decrease with increasing polymer concentrations, leveling off at concentrations above 1.0 wt % (Figure 9). At low polymer concentration (0.05 wt %), the phase transition occurs over a broad temperature range (Figure 8). These observations are in agreement with the following considerations: the thermally induced phase separation of aqueous polymer solutions has been proposed to take place in two stages, with individual polymer chains first forming primary aggregates, which then macroscopically aggregate to cause phase separation.[34] The primary aggregates require higher temperatures before aggregating macroscopically. Higher polymer concentrations would also shift this equilibrium, causing the cloud point to occur at a lower temperature. Compared to the liquid−solid phase transition of pNIPAM solution,[33,35] the effect of polymer concentration on the phase transition temperature of DMA-*co*-PhAm solution is hence more pronounced. Similar observations were reported for the liquid−liquid phase transition of elastin-like polypeptide solutions.[36,37]

It is well-known that the effect of salts on the cloud point is mainly due to the resulting changes in the structure of water.[32,38] As shown in Figure 10, the cloud point temperature of DMA-*co*-PhAm solutions decreases with the addition of NaCl. NaCl is considered as a water structure maker and hence shows a "salting-out" effect, which can effectively enhance the hydrophobic interaction and promote the collapse of polymer chains.

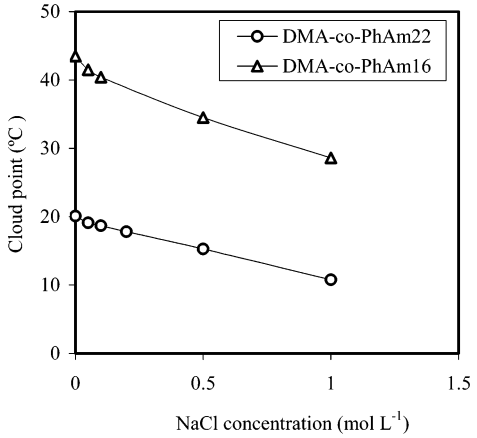

Figure 10. Effect of NaCl concentration on the phase separation temperature of 1.0 wt % DMA-*co*-PhAm solutions as measured by the cloud point method.

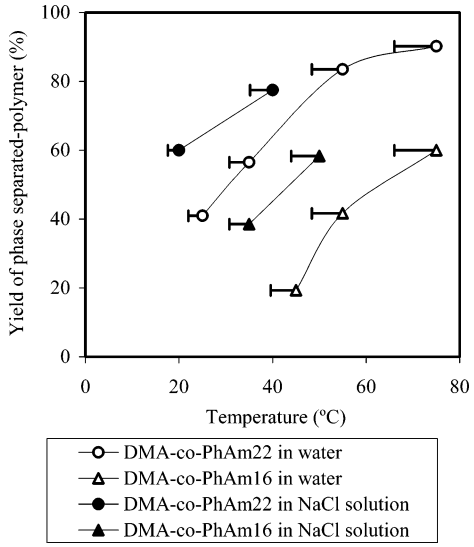

Figure 11. Effect of temperature on the yield of phase-separated polymer from 2.0 wt % DMA-*co*-PhAm copolymer aqueous solutions and in 1.0 mol L^{-1} NaCl solutions. The symbols indicate the equilibrium temperature, and the error bars show the decrease of temperature during centrifugation.

Efficiency of Phase Separation. The efficiency of the thermally induced liquid−liquid phase separations was investigated by determining the yield of polymer recovered from the coacervate phase at different temperatures above the cloud points. Figure 11 shows the percentage of the polymer found in the coacervate phase to increase with increasing temperature. Compared to our previously studied copolymers of DMA with glycidyl methacrylate[16] and allyl methacrylate,[17] the yields of the present DMA−PhAm copolymers are much higher near the onset of phase transition. The polymers used in the previous work were prepared by conventional free radical polymerization and subsequently had broad distributions of polymer molecular weights. Though based on different hydrophobic comonomers, the present results suggest that the efficiency of the phase transition can be increased by using narrow-disperse polymers. Furthermore, the temperature-dependent efficiency of phase separation, even for narrow-disperse copolymers, confirms that the thermally induced liquid−liquid phase separation is an equilibrium process. In this process, only part of the polymer chains are dehydrated upon reaching the cloud point temperature, and higher temperatures are required to drive more polymer to the coacervate phase.

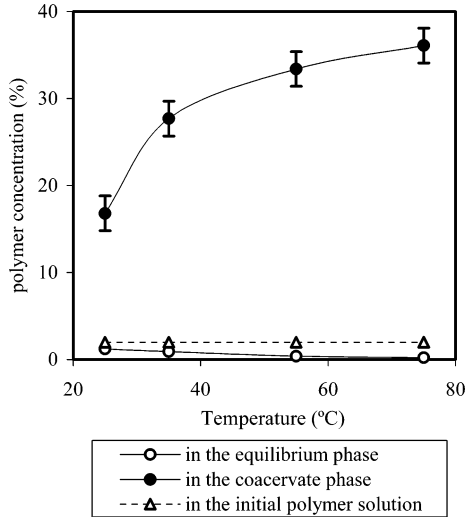

Figure 12. Concentrations of DMA-*co*-PhAm22 in the two separated phases at different temperatures.

Figure 12 shows the concentration of DMA-*co*-PhAm22 in the two separated phases as a function of temperature. The temperature changes do not affect the volume of the two separated phases. Hence, the concentrations of polymer in the coacervate phase increase with increasing temperatures. The water content in the coacervate phase is however still larger than 60% at 75 °C.

The polymers recovered from both phases were characterized by GPC and NMR and were found to have similar compositions and molecular weights.

As discussed above, the cloud point temperatures decrease upon addition of NaCl to the solutions. Also illustrated in Figure 11 is the effect of NaCl addition on the efficiency of the phase separation. During the polymer recovery, it was assumed that NaCl is present in equal concentrations in both the polymer-poor and the polymer-rich (coacervate) phases. With the addition of NaCl, the volume of both separated phase does not change, while the efficiency of phase separations is enhanced.

Conclusions

pDMA homopolymer and DMA-*co*-PhAm copolymers were synthesized by ATRP using MCP/CuCl/Me_6TREN as the initiator and the catalyst at room temperature, with the hydrogen-bonding methanol and methanol/water mixtures as the reaction media. The polymerizations were well controlled, leading to the production of DMA-*co*-PhAm copolymers with well-defined structures and compositions.

Aqueous solutions of DMA-*co*-PhAm copolymers showed liquid−liquid phase separations at temperatures dependent on the content of hydrophobic PhAm. These cloud points were also found to depend on the polymer concentrations and molecular weights. The efficiency of the thermally induced liquid−liquid phase separation was studied by measuring the yield of phase-separated polymers, which increased with increasing temperature. This temperature dependence of the phase separation efficiency showed the thermally induced liquid−liquid phase separation to be an equilibrium process. The polymer chains only partially dehydrate upon reaching the cloud point, and the solubility of

polymers in the equilibrium phase progressively decreased with increasing temperature, leading to more polymers driven from the continuous to the coacervate phase. The addition of NaCl further enhances the efficiency of phase separation without changing the water content in the separated phases.

Acknowledgment. We thank Dr. Nicholas Burke for valuable discussions, Yan Xia for assistance with the ^{1}H NMR, Professor P. Berti for the use of the variable temperature Cary 50 UV/vis instrument, and the Natural Sciences and Engineering Research Council of Canada and 3M Canada Company for financial support.

References and Notes

(1) Albertsson, P-Å. *Partition of Cell Particles and Macromolecules*, 3rd ed.; J. Wiley & Sons: New York, 1986.
(2) Li, M.; Zhu, Z. Q.; Mei, L. H. *Biotechnol. Prog.* **1997**, *13*, 105−108.
(3) Johansson, H.-O.; Karlström, G.; Tjerneld, F.; Haynes, C. A. *J. Chromatogr., B* **1998**, *711*, 3−17.
(4) Abbott, N. L.; Blankschtein, D.; Hatton, T. A. *Macromolecules* **1991**, *24*, 4334−4348.
(5) Carlsson, M.; Linse, P.; Tjerneld, F. *Macromolecules* **1993**, *26*, 1546−1554.
(6) Persson, J.; Nyström, L.; Ageland, H.; Tjerneld, F. *J. Chromatogr., B* **1998**, *711*, 97−109.
(7) Johansson, H.-O.; Karlström, G.; Tjerneld, F. *Macromolecules* **1993**, *26*, 4478−4483.
(8) Johansson, H.-O.; Persson, J.; Tjerneld, F. *Biotechnol. Bioeng.* **1999**, *66*, 247−257.
(9) Urry, D. W. *J. Phys. Chem. B* **1997**, *101*, 11007−11028.
(10) Meyer, D. A.; Chilkoti, A. *Nat. Biotechnol.* **1999**, *17*, 1112−1115.
(11) Zhang, Y.; Mao, H.; Cremer, P. S. *J. Am. Chem. Soc.* **2003**, *125*, 15630−15635.
(12) Schild, H. G. *Prog. Polym. Sci.* **1992**, *17*, 163−249.
(13) Mueller, K. F. *Polymer* **1992**, *33*, 3470−3476.
(14) Miyazaki, H.; Kataoka, K. *Polymer* **1996**, *37*, 681−685.
(15) Shibanuma, T.; Aoki, T.; Sanui, K.; Ogata, N.; Kikuchi, A.; Sakurai, Y.; Okano, T. *Macromolecules* **2000**, *33*, 444−450.
(16) Yin, X.; Stöver, H. D. H. *Macromolecules* **2003**, *36*, 9817−9822.
(17) Yin, X.; Stöver, H. D. H. *J. Polym. Sci., Part A: Polym. Chem.*, in press.
(18) Matyjaszewski, K.; Xia, J. *Chem. Rev.* **2001**, *101*, 2921−2990.
(19) Ciampolini, M.; Nardi, N. *Inorg. Chem.* **1966**, *5*, 41−44.
(20) Teodorescu, M.; Matyjaszewski, K. *Macromolecules* **1999**, *32*, 4826−4831.
(21) Rademacher, J. T.; Baum, M.; Pallack, M. E.; Brittain, W. J.; Simonsick, W. J. *Macromolecules* **2000**, *33*, 284−288.
(22) Teodorescu, M.; Matyjaszewski, K. *Macromol. Rapid Commun.* **2000**, *21*, 190−194.
(23) Neugebauer, D.; Matyjaszewski, K. *Macromolecules* **2003**, *36*, 2598−2603.
(24) Xia, J.; Zhang, X.; Matyjaszewski, K. *Macromolecules* **1999**, *32*, 3531−3533.
(25) Lutz, J.; Neugebauer, D.; Matyjaszewski, K. *J. Am. Chem. Soc.* **2003**, *125*, 6986−6993.
(26) Wang, X. S.; Armes, S. P. *Macromolecules* **2000**, *33*, 6640−6647.
(27) Robinson, K. L.; Khan, M. A.; de Paz Báñez; M. V.; Wang, X. S.; Armes, S. P. *Macromolecules* **2001**, *34*, 3155−3158.
(28) Takei, Y. G.; Aoki, T.; Sanui, K.; Ogata, N.; Okano, T.; Sakurai, Y. *Bioconjugate Chem.* **1993**, *4*, 341−346.
(29) Feil, H.; Bae, Y. H.; Feijen, J.; Kim, S. W. *Macromolecules* **1993**, *26*, 2496−2500.
(30) Shibayama, M.; Mizutani, S.; Nomura, S. *Macromolecules* **1996**, *29*, 2019−2024.
(31) Fujishige, S.; Kubota, K.; Ando, I. *J. Phys. Chem.* **1989**, *93*, 3311−3313.
(32) Schild, H. G.; Tirrell, D. A. *J. Phys. Chem.* **1990**, *94*, 4352−4356.
(33) Tong, Z.; Zeng, F.; Zheng, X.; Sato, T. *Macromolecules* **1999**, *32*, 4488−4490.
(34) Qiu, X.; Wu, C. *Macromolecules* **1997**, *30*, 7921−7926.
(35) Otake, K.; Inomata, H.; Konno, M.; Saito, S. *Macromolecules* **1990**, *23*, 283−289.
(36) Nagarsekar, A.; Crissman, J.; Crissman, M.; Ferrari, F.; Cappello, J.; Ghandehari, H. *Biomacromolecules* **2003**, *4*, 602−607.
(37) Yamaoka, T.; Tamura, T.; Seto, Y.; Tada, T.; Kunugi, S.; Tirrell, D. A. *Biomacromolecules* **2003**, *4*, 1680−1685.
(38) Park, T. G.; Hoffman, A. S. *Macromolecules* **1993**, *26*, 5045−5048.

MA048853P